Applied Catalysis B: Environmental 92 (2009) 75–89

Contents lists available at ScienceDirect

Applied Catalysis B: Environmental

journal homepage: www.elsevier.com/locate/apcatb

Hydrolysis and oxidation of gaseous HCN over heterogeneous catalysts

O. Kröcher *, M. Elsener

Paul Scherrer Institute, 5232 Villigen PSI, Switzerland

ARTICLE INFO

Article history:
Received 2 June 2009
Received in revised form 10 July 2009
Accepted 20 July 2009
Available online 28 July 2009

Keywords:
HCN hydrolysis
HCN oxidation
Heterogeneous catalysts
SCR
TWC

ABSTRACT

The hydrolysis and oxidation of HCN, which is a potential toxic emission of automotive catalysts, were systematically examined with model gas experiments on typical hydrolysis, SCR and oxidation catalysts.

TiO_2-anatase showed the highest HCN hydrolysis activity among the hydrolysis catalysts, with approximately two times more activity than Al_2O_3. On Fe-ZSM-5, HCN was converted to NH_3 to the same degree as on TiO_2. In the presence of NO_x, the NH_3 formed from HCN reacted in the SCR reaction to form nitrogen.

On Pd- and Pt-containing oxidation catalysts, which are used in SCR systems as ammonia slip catalysts, HCN is converted with very high activity above 250–300 °C. The same reaction products are formed as in the oxidation of NH_3, i.e., aside from nitrogen N_2O and NO_x appear as unwanted reaction products depending on the temperature and gas composition. Similarly high HCN conversions, but clearly better N_2 selectivities, were reached on Cu-ZSM-5 and MnO_x-Nb_2O_5-CeO_x.

The precise measurement of all relevant gas components allowed us to develop a reaction scheme for the HCN decomposition chemistry over a variety of heterogeneous catalysts. Over hydrolyzing catalysts water interacts with HCN, forming methanamide and then ammonium formate, which decomposes to ammonia and formic acid. The formic acid finally thermolyzes to water and CO. Catalysts with oxidizing properties oxidize HCN to HNCO in the first reaction step, which then hydrolyzes to unstable carbamic acid. Carbamic acid decomposes to CO_2 and NH_3, which can be further oxidized to N_2, N_2O or NO_x. The oxidation of HCN to HNCO may also proceed with $(CN)_2$ as an intermediate over Pd-, Pt- and Cu-containing catalysts.

1. Introduction

The application of catalysts for cleaning the exhaust gases of internal combustion engines of CO, hydrocarbons, NO_x and particle emissions does not only yield water, CO_2 and nitrogen as desired harmless reaction products, but may also produce unwanted side-products, such as NO_2, N_2O or HCN, among others. In this study, we focus on HCN emissions, which must be considered as a potential emission from the well-established three-way-catalyst (TWC) [1], as well as from new exhaust gas treatment technologies. As new technology that is still at the research stage, the selective catalytic reduction of NO_x with hydrocarbons (HC-SCR) must be mentioned, for which HCN emissions have been reported [2,3]. Another relatively new technology is the urea–SCR process, in which ammonia reduces NO_x over a catalyst in a very selective reaction. Although HCN emissions do not occur in this process, when urea solution was used as the reducing agent, we observed the formation of HCN in investigations of alternative ammonia precursor compounds with deeper freezing points and better stability at elevated temperatures [4,5]. It was observed that the formation of HCN was especially pronounced when formic acid was also present or with formate-containing reducing agents such as ammonium formate and guanidinium formate. HCN was also found in experiments with methanamide as the SCR reducing agent. HCN formation usually remains at a low ppm level, but it can reach higher concentrations of a few hundred ppm during unfavorable hydrolysis conditions.

Formate-containing N-reducing agents, such as ammonium formate, guanidinium formate or methanamide, produce ammonia and formic acid during decomposition, from which HCN may be formed by the dehydration of ammonium formate over methanamide as intermediate products according to the following reaction sequence [4,5]:

$$NH_3 + HC(O)OH \rightarrow HC(O)ONH_4 \quad (1)$$

$$HC(O)ONH_4 \rightarrow HC(O)NH_2 + H_2O \quad (2)$$

$$HC(O)NH_2 \rightarrow HCN + H_2O \quad (3)$$

The formation of methanamide from NH_3 and HC(O)OH may also be formulated as direct amidation reaction without ammonium formate as intermediate.

* Corresponding author. Tel.: +41 56 310 20 66; fax: +41 56 310 21 99.
E-mail address: oliver.kroecher@psi.ch (O. Kröcher).

0926-3373/$ – see front matter © 2009 Elsevier B.V. All rights reserved.
doi:10.1016/j.apcatb.2009.07.021

In order to avoid toxic HCN emissions from exhaust post-treatment systems, catalytic oxidation (4) or hydrolysis (5) of HCN downstream of the HCN-generating catalyst would be an attractive solution:

$$4HCN + 5O_2 \rightarrow 4CO_2 + 2N_2 + 2H_2O \quad (4)$$

$$HCN + H_2O \rightarrow NH_3 + CO \quad (5)$$

Only a few publications could be found focused on the catalytic decomposition of HCN in the gas phase. The first study we found was reported by Carpenter and Linder in 1905; they used brick, iron oxide and Weldon mud to hydrolyze HCN to ammonia [6]. In 1952, Marsh et al. demonstrated that Al_2O_3 may be used to hydrolyze HCN in oxygen-free off-gas streams at 400 °C [7]. HCN may also be removed by using it as an SCR reducing agent in the reaction with NO_x. This concept was attempted by Miyadera, who tested Pt, Pd, Rh, Ag, V_2O_5, WO_3 and $CuSO_4$, each supported on TiO_2 pellets, as catalysts in this reaction [8]. $CuSO_4/TiO_2$ proved to be the most active catalyst, but all catalysts produced significant N_2O emissions, which made this approach rather unattractive.

In a practice-oriented study, Hoard and Panov mentioned that HCN emissions formed during plasma-assisted HC-SCR can be removed over a commercial platinum-based oxidation catalyst [9]. A detailed investigation of the HCN oxidation reaction over a Pt/Al_2O_3 catalyst was carried out by Peden and co-workers [10]. They found N_2, N_2O, NO, NO_2, CO_2 and H_2O as reaction products, but no NH_3 and CO due to the strongly oxidizing conditions applied. CN^{ads} was identified as a strongly bound reaction intermediate, which was completely oxidized above 400 °C. There is evidence in the literature that cyanogen $(CN)_2$ is easily formed on Pt (1 1 1) and Pt (1 1 2) single crystal surfaces from CN^{ads} [11,12], but the production of considerable amounts of cyanogen $(CN)_2$, which could not be measured with the applied analytics, was ruled out on basis of the good carbon balance observed for the other reaction components. A mechanism for the oxidation of HCN over platinum-based oxidation catalysts was suggested to proceed via dissociation into H^{ads} and CN^{ads}, which is oxidized by O^{ads} to surface isocyanate (NCO^{ads}). The isocyanate decomposes to N^{ads} and CO^{ads}, which are stepwise oxidized to the final desorbing species NO, NO_2 and CO_2.

The possible formation of cyanogen must always be considered when HCN and oxygen are brought in contact over heterogeneous catalysts, since a variety of industrial processes have been developed that involve a gas phase reaction of HCN and O_2 over a solid catalyst to produce C_2N_2 in high yields [13]. Cu-based catalysts seem to be especially suited for this reaction.

Additionally, zeolites may be used to hydrolyze HCN. Nanba et al. found that H-ferrierite coated on cordierite monoliths (400 cpsi) converted about 78% of 250 ppm HCN at a GHSV of 21,200 h^{-1} and a temperature of 500 °C in the presence of water and oxygen [14]. The main reaction was the hydrolysis of HCN to ammonia and CO, but above 400 °C, small amounts of CO_2 were also found, pointing to the partial oxidation of HCN above this temperature. In the presence of NO_x, the NH_3 formed from the hydrolysis of HCN was consumed in the SCR reaction, yielding N_2 and N_2O.

The formation and decomposition of HCN is of special interest for the HC-SCR process, since HCN is formed in significant amounts as a side-product of this process over metal-exchanged zeolites. Cant et al. studied the reaction pathways of methanamide as important intermediate in the HC-SCR chemistry over Co-ZSM-5 [15]. They concluded that methanamide decomposes under water-free conditions to HCN and water, which react further to form ammonia and CO, or that the HCN formed may be oxidized to N_2, CO_2 and water. The reaction was also tested with water in the feed, and an increase in ammonia and CO production was observed. The authors speculated that the hydrolysis of HCN might proceed via methanamide and ammonium formate as intermediates, i.e., the reverse of Eqs. (3) to (1), followed by the decarbonylation of formic acid to ammonia and CO (6), by which formic acid is withdrawn from the equilibria.

$$HC(O)OH \rightarrow CO + H_2O \quad (6)$$

However, no further evidence could be provided for this mechanism, since formic acid and methanamide could not be measured. It was suggested that the zeolite catalyst may act as a Brønsted acid in this reaction sequence, facilitating the protonation of methanamide, which then deaminates to form ammonium and formic acid. The formation and reactions of HCN were also investigated over Cu- and Fe-ZSM-5 by the same authors [16–18]. Both catalysts showed high intrinsic activity for the conversion of HCN to nitrogen: Fe-ZSM-5 mainly by hydrolysis and Cu-ZSM-5, to a large extent, by oxidation. Remarkably, over Cu-ZSM-5, the formation of $(CN)_2$ was observed under water-free conditions, which is in line with the application of Cu-based catalysts for the industrial production of this compound [13].

The HCN emissions found during the decomposition of methanamide and guanidinium formate for non-optimum reaction conditions, as well as the observed HCN emissions during HC-SCR, motivated us to investigate the catalytic hydrolysis or oxidation of HCN under practice-oriented conditions, with the aim of finding new and improved catalysts for these reactions. In this respect, the present study differs from previous investigations, which dealt only with a small selection of catalysts or tried to answer specific mechanistic questions. In particular, we examined (a) the hydrolysis of HCN on different metal oxide catalysts, (b) the behavior of HCN on typical SCR catalysts and (c) the oxidation of HCN on noble-metal-based ammonia oxidation catalysts. In real diesel exhaust gases, changes in the concentrations of NO, NO_2 or NH_3 may occur, so the influence of these components on HCN decomposition was also investigated, particularly on the formation of additional by-products such as N_2O.

For the assessment of the catalytic materials, two possible positions and functions in the SCR system must be distinguished: (a) If HCN degradation takes place on an upstream hydrolysis catalyst or on the SCR catalyst itself, the HCN hydrolysis rate to NH_3 should be as high as possible, also in the presence of high ammonia concentrations. The catalyst must not exhibit ammonia oxidation with oxygen, since this would lead to an unwanted overconsumption of the reducing agents. (b) When HCN is oxidized downstream of an SCR catalyst, the aim is complete oxidation to N_2, CO_2 and H_2O. The formation of unwanted secondary emissions such as NH_3, N_2O, NO_x, formic acid, CO, HNCO or methanamide should be as small as possible.

2. Experimental methods

2.1. Catalyst specifications

The specifications of the tested catalysts are listed in Table 1. The commercial catalysts, i.e., the Cu-ZSM-5 catalyst, the Pt/Al_2O_3-based diesel oxidation catalyst and the V_2O_5/WO_3-TiO_2 catalyst, later impregnated with platinum, were sawn out of larger monoliths. The other modules were manufactured by the coating of cordierite monoliths with commercial or in-house prepared catalyst powders. Therefore, the catalyst powders were dispersed in water and coated on the monoliths by repeated immersing and intermediate drying until the desired catalyst quantity was reached. 10 wt.% Ludox (colloidal ammonium silicate solution) related to the catalyst mass was added to the dispersion as an inorganic binder. The coated monoliths were finally calcined at 550 °C in air for 5 h.

Table 1
Catalyst specifications and measuring conditions.

Catalyst	Details	Mass (g)	Monolith volume (cm^3)	Catalyst loading (g/L)	GHSV (h^{-1})	Gas flow (L_N/h)
TiO_2	Anatase modification, DT51 from Millenium Chem.	1.28	8.54	150	52000	444
Al_2O_3	Boehmite, Dispersal S from Sasol, Calcined at 550 °C for 5 h	1.28	8.54	150	52000	444
ZrO_2	Zr(IV)-oxide <5 μm, Aldrich 230693	1.18	8.54	138	52000	444
SiO_2	Aerosil 200 from Degussa	1.10	8.54	129	52000	444
La_2O_3-TiO_2	TiO_2 (anatase) with La_2O_3, DT57 from Millenium Chem.	1.00	8.54	117	52000	444
WO_3-TiO_2	TiO_2 (anatase) with 9.6% WO_3, DT52 from Millenium Chem.	1.24	8.54	145	52000	444
MoO_3/TiO_2	3.6% MoO_3 on DT51	1.38	8.49	163	52000	442
Fe_2O_3/TiO_2	3.6% FeO_x on DT51	1.16	8.28	140	52000	431
V_2O_5/WO_3-TiO_2	2.3% V_2O_5 on DT52, prepared in-house [19]	1.32	8.43	157	52000	439
H-ZSM-5	Süd-Chemie	0.90	8.43	107	52000	439
Fe-ZSM-5	Süd-Chemie	1.03	8.54	121	52000	444
Cu-ZSM-5	Umicore	ca. 0.3	2.32	ca. 130	200000	465
Pd/Al_2O_3	1% Pd on Al_2O_3	0.31	2.37	131	200000	474
Pt/Al_2O_3	1% Pt on Al_2O_3	0.31	2.42	129	200000	483
$Pt/V_2O_5/WO_3$-TiO_2	Extruded commercial catalyst with ca. 2.5% V_2O_5 from Ceram, in-house impregnation with 1% Pt	1.65	2.29	719	200000	459
Comm. DOC	Commercial diesel oxidation catalyst with 90 g Pt/ft^3 on Al_2O_3, Umicore	ca. 0.25	2.25	ca. 110	200000	450
MnO_x-Nb_2O_5-CeO_2	Mn:Nb:Ce = 23:23:54 (mol%) made in-house [20]	0.34	2.32	145	200000	465

2.2. Experimental setup and analysis

All catalytic tests in the laboratory were carried out with coated cordierite monoliths with a cell density of 400 cpsi. The measurements were performed with model gases at a space velocity of 52,000 h^{-1} at STP with modules with a frontal area of 1.2 cm × 1.7 cm (9 × 13 cells) and a length of approximately 40 mm. Highly active oxidation catalysts were measured with smaller monoliths at a space velocity of 200,000 h^{-1} at STP. Details of the catalysts, such as catalyst volume, composition of the active mass, catalyst loading and space velocity, are specified in Table 1.

The model gas flow was composed of nitrogen with 10% O_2, 5% H_2O and 50 ppm HCN with changing admixtures of 200 ppm NO, 100 ppm NO and NO_2, 200 ppm NO_2 or 200 ppm NH_3. Some catalysts were examined only with 5% H_2O or 10% O_2 in order to better identify whether HCN was degraded by a hydrolytic or oxidative reaction path. HCN, NO, NO_2 and NH_3 were dosed from higher concentrated gas mixtures (0.5–5% in N_2) obtained from carbagas and water was brought into the gas phase by an electrically heated evaporator.

For the analysis of the product gas mixture, an FTIR spectrometer equipped with a heated 2-m gas measuring cell (model Nexus from Thermo Fisher) was used at a resolution of 0.5 cm^{-1}. A multi-component gas analysis method was developed, which corrects non-linear responses and cross-sensitivities. In Table 2, the measured components with their detection limits are specified. Although the absorption coefficient of CO_2 is larger than that of CO, its detection limit is higher due to atmospheric CO_2, which penetrated the spectrometer through unavoidable leaks. Methanamide and formaldehyde were not found in the measurements, so they are not specified in the resultant tables and figures. Isocyanic acid was only found in traces much below 1 ppm in some measurements, which was a too low concentration to be evaluated. However, in the step-response experiments with Cu-ZSM-5 the stepwise change of the very low HNCO concentration could be reliably measured.

Table 2
Gas components measured by FTIR spectroscopy and their detection limits.

Components		Detection limit (ppm)
Hydrocyanic acid	HCN	0.2
Carbon monoxide	CO	0.2
Carbon dioxide	CO_2	1–2
Formic acid	HC(O)OH	0.2
Isocyanic acid	HNCO	0.2
Methanamide	$HC(O)NH_2$	0.5
Formaldehyde	H_2CO	1
Nitric oxide	NO	1
Nitrogen dioxide	NO_2	1
Nitrous oxide	N_2O	0.1
Ammonia	NH_3	0.2
Nitric acid	HNO_3	1

2.3. Carbon balances and N_2 formation

In the evaluation of the measurement quality, the carbon balances after catalysis are important, which supply information about non-identified and non-measured by-products. The observed C-balances were usually very close to the C-feed concentrations of 50 ppm. Deviations were observed for some individual measurements, particularly when the catalyst temperatures were low and when catalysts with large storage capacities were used, with which the equilibrium over the catalyst was slowly reached.

The N-balances were also very good for the pure hydrolysis catalysts, with exclusive formation of NH_3 as the N-containing reaction product and, for the very strong oxidation catalysts, with complete oxidation of the HCN nitrogen to NO_x or N_2O. With the other catalyst types, N_2 is formed as a reaction product over the SCR or during the NH_3 oxidation reaction, depending on the model gas composition. Although N_2 is not detectable by FTIR spectroscopy, N_2 formation can be calculated from the N-balances due to the high measuring accuracy of the remaining N-containing reaction products of ±2%. The manual evaluation of selected FTIR spectra did not show any additional non-identified by-products.

$$C_{N_2} = \frac{C_{N\_in} - C_{NO_{x}\_out} - C_{NH_3\_out} - C_{HCN_{out}}}{2} - C_{N_2O_{out}} \quad (7)$$

2.4. Selectivities

The selectivities of HCN decomposition can be divided into reaction paths with C- and N-containing reaction products. Since HCN is the only C-containing component in the model gas, the C-involving reaction paths can always be reliably calculated from the reaction products, whereas this is not always or only indirectly possible for the N-involving reaction paths when NO_x or NH_3 are simultaneously dosed. In particular, for the combination of small HCN conversions with an additional dosage of NO_x or NH_3, large

errors may result from the sum of dosages and measuring uncertainties.

The selectivity of the C-containing product x (x = CO, CO_2, formic acid, methanamide, HNCO) was obtained from the converted amount of HCN and the amount of x (8):

$$S_x = \frac{C_x}{(C_{HCN_{in}} - C_{HCN_{out}})} \quad (8)$$

Without an additional dosage of N-containing gases (NO_x or NH_3), the selectivities of the reaction paths in the HCN decomposition were calculated as follows (9)–(12):

$$S_{NH_3} = \frac{C_{NH_3\_out}}{(C_{HCN_{in}} - C_{HCN_{out}})} \quad (9)$$

$$S_{N_2} = 2\frac{C_{N_2\_out}}{(C_{HCN_{in}} - C_{HCN_{out}})} \quad (10)$$

$$S_{N_2O} = 2\frac{C_{N_2O\_out}}{(C_{HCN_{in}} - C_{HCN_{out}})} \quad (11)$$

$$S_{NO_x} = \frac{C_{NO_x\_out}}{(C_{HCN_{in}} - C_{HCN_{out}})} \quad (12)$$

When NO_x or NH_3 was dosed, the selectivities of the HCN decomposition could not be easily determined. In the case of NH_3 dosage, ammonia formation from HCN can theoretically be calculated for pure hydrolysis catalysts from the ammonia balance. For small HCN conversions and correspondingly small NH_3 formations, the measuring uncertainty became very large due to the high NH_3 background signal. For the oxidation catalysts, the N in NH_3 oxidizes to the same reaction products as the N in HCN, and thus, a determination of the reaction paths was not possible.

When NO_x was dosed, it could not be differentiated from the reaction products N_2O and N_2 in terms of whether both N-atoms came from HCN or whether one came from NO_x, reduced by NH_3 from hydrolyzed HCN. Since the primary intention of the calculations was to reveal the influence of NO_x on the formation of unwanted by-products (N_2O), we adhered to the definition of the selectivities S_{NH_3}, S_{N_2} and S_{N_2O} given by Eqs. (11)–(13). It should be noted that due to the additional N from the reaction of NO_x with the HCN nitrogen, the sum of the selectivities may exceed 100%.

When NO_x was dosed, the formation of NO_x from the oxidation of HCN could only be proven when NO_{x_out} was larger than NO_{x_in} (13). Otherwise, S_{NO_x} was set to zero, even under consideration of the probable intermediate formation of NO_x followed by its reduction to N_2 or N_2O (14).

$$\text{if } NO_{x\_out} > NO_{x\_in}: \quad S_{NO_x} = \frac{(C_{NO_{x\_out}} - C_{NO_{x\_in}})}{(C_{HCN_{in}} - C_{HCN_{out}})} \quad (13)$$

$$\text{if } NO_{x\_out} \leq NO_{x\_in}: \quad S_{NO_x} = 0 \quad (14)$$

3. Results

3.1. Metal oxides

3.1.1. HCN conversion rates

In Table 3, the mass-based reaction rate constants of HCN conversion over TiO_2, Al_2O_3, ZrO_2 and SiO_2 in the presence of 5% H_2O and 10% O_2 are given. In Fig. 1, the rate constants measured over these four metal oxides are represented as Arrhenius plots. On TiO_2, the highest HCN conversions were obtained over a large temperature range, but the clear decrease in conversion at temperatures above 400 °C is remarkable. A linear temperature dependence of the rate constants is only found between 200 and 300 °C. Above 300 °C, the curve levels off, which can only be partly explained by diffusion limitations, which start to occur for rate constants from 200 to 400 $cm^3/(g\ s)$ [21]. The pronounced leveling off, and especially the decrease in the rate constant from 505 $cm^3/(g\ s)$ at 400 °C to only 279 $cm^3/(g\ s)$ at 500 °C, is most likely caused by a substantial decrease in the surface coverage by one or both of the reactants H_2O and HCN [22].

Table 3
Mass-based reaction rate constants at STP of HCN decomposition over different metal oxide catalysts in the presence of 5% H_2O and 10% O_2.

$T_{cat.}$ (°C)	k_{mass} ($cm^3/(g\ s)$)			
	TiO_2	Al_2O_3	ZrO_2	SiO_2
500	279	518	81	20
450	438	458	83	18
400	504	339	64	11
350	439	181	30	10
300	306	78	18	10
250	101	24	12	9
200	25	10	7	–

On Al_2O_3, clearly lower HCN conversions were reached than on TiO_2 up to 400 °C, but a more moderate leveling off of the reaction rates was observed. Moreover, a decrease in the rates at higher temperatures was not observed. The adsorption behavior of both reactants seems to be more favorable on Al_2O_3 than on TiO_2 at very high temperatures, but the reaction rates of HCN conversion are two to four times lower in the temperature range of 200–400 °C, which is the most relevant for automotive catalysis.

ZrO_2 showed low hydrolysis activity, and SiO_2 showed almost no HCN hydrolysis activity. The weakly acidic ZrO_2 is clearly inferior to the amphoteric TiO_2 and Al_2O_3 with respect to HCN hydrolysis. In our previous studies of the hydrolysis of HNCO, however, the activity of ZrO_2 was equivalent to that of the two other oxides and even exceeded it, at temperatures below 150 °C [23].

3.1.2. Influence of the model gas composition

The model gas composition has only a small influence on the rate of HCN conversion over the different single metal oxides. The performances of TiO_2 and Al_2O_3 were virtually the same, and the reaction showed little change on the low-activity catalysts ZrO_2 and SiO_2. The addition of NO, NO_2 and NH_3 generally showed only a small influence on the HCN decomposition rate, and the deviations were usually in the range of the measuring uncertainties. Only NO_2 and NH_3 showed a small inhibiting effect at low temperatures.

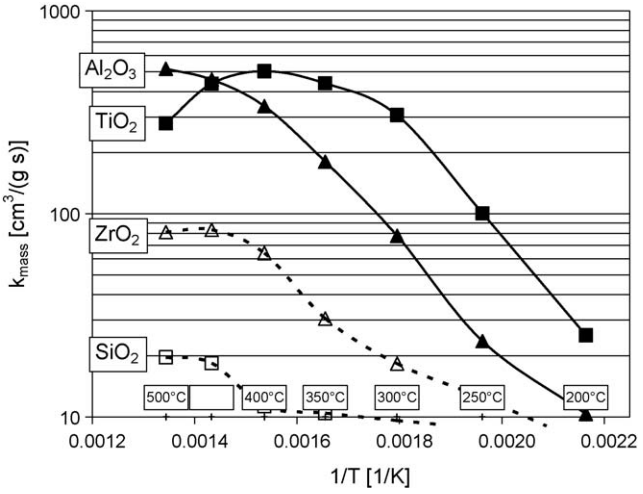

Fig. 1. Reaction rate constants at STP of HCN decomposition over TiO_2, Al_2O_3, ZrO_2 and SiO_2. Model gas: 5% H_2O, 10% O_2 and 50 ppm HCN in N_2.

Table 4
Influence of the model gas composition on the formation of CO, CO_2 and formic acid and on the selectivity of HCN decomposition over TiO_2.

$T_{cat.}$ (°C)	$O_2 + H_2O$			$O_2 + H_2O + NO$			$O_2 + H_2O + NO_2$		
	CO (ppm)	CO_2 (ppm)	Formic acid (ppm)	CO (ppm)	CO_2 (ppm)	Formic acid (ppm)	CO (ppm)	CO_2 (ppm)	Formic acid (ppm)
500	30	2	<0.5	29	1	<0.5	29	3	<0.5
450	39	1	<0.5	39	1	<0.5	38	3	<0.5
400	44	2	<0.5	45	1	<0.5	44	2	<0.5
350	44	1	<0.5	44	1	<0.5	43	3	<0.5
300	38	1	0.7	39	1	0.7	37	1	0.7
250	15	1	2	16	1	2	16	1	2
200	1	1	1	–	–	–	–	–	–

$T_{cat.}$ (°C)	$O_2 + H_2O$			$O_2 + H_2O + NO$			$O_2 + H_2O + NO_2$		
	NH_3 (ppm)	S_{NH_3} (%)	N_2 (ppm)	NH_3 (ppm)	S_{NH_3} (%)	N_2 (ppm)	NH_3 (ppm)	S_{NH_3} (%)	N_2 (ppm)
500	29	91	1	20	67	7	17	55	7
450	39	95	1	32	80	6	30	77	4
400	43	98	1	39	88	3	35	81	7
350	42	97	1	41	95	1	35	82	5
300	36	92	2	37	95	1	30	86	9
250	19	90	1	17	77	1	4	21	19
200	6	(85)	1	–	–	–	–	–	–

In the following, we report the influence of the model gas composition on TiO_2, which proved to be the most efficient HCN hydrolysis catalyst. With only 10% O_2 in the feed, HCN was not converted below 400 °C (data not shown, see electronic supporting information). Even above this temperature, the observed typical hydrolysis products NH_3 and CO point to traces of water in the model gas feed rather than to an oxidation reaction. However, above 500 °C, traces of the typical oxidation products NO and CO_2 were found. For the formation of CO_2, an oxidizing step is necessary, which is only feasible on this material at very high temperatures.

With O_2 and H_2O in the feed, mainly NH_3 and CO were produced (Table 4, Fig. 2a), in line with the hydrolysis of HCN according to Eq. (5). The 1–2 ppm of formic acid formed at low temperatures points to a two-stage mechanism: first, water was added to HCN to form methanamide as an intermediate, which hydrolyzed to NH_3 and formic acid, which is in line with the reverse of the methanamide decomposition over TiO_2 [4,5] and the suggestion of Cant et al. for HCN hydrolysis over metal-exchanged zeolites [15]. For such a mechanism, one may expect the formation of CO_2 at low temperatures due to the decarboxylation of formate, which was observed for the decomposition of ammonium formate (Denoxium) and methanamide at very low temperatures [4,5]. However, in this study, decarboxylation could not be detected within the measurement uncertainty due to the small HCN conversions at low temperatures.

The selectivity of the ammonia formation on TiO_2 was near 100%, as expected. With NO in the model gas, some SCR with NH_3 was observed at high temperatures under the formation of N_2, which reflects the low SCR activity of this material (Fig. 2b). The typical products of oxidation reactions, NO_2, N_2O or CO_2, were not observed. With NO_2 in the feed, the SCR reaction took place, even at the relatively low temperature of 250 °C (data not shown, see electronic supporting information).

3.2. Doped titania

Since TiO_2 exhibited the best hydrolysis properties of all of the investigated single metal oxides, experiments with the following doped TiO_2 materials were also carried out.

La_2O_3-TiO_2 is a basic titanium oxide on which the weakly acidic HCN might be more strongly adsorbed, even at higher temperatures, and the basic reaction product NH_3 might be more easily desorbed. WO_3-TiO_2 is often used as a starting material for the production of vanadia-based SCR catalysts. It exhibits an acidic surface due to doping with WO_3. V_2O_5/WO_3-TiO_2 is a well-established vanadia-based SCR catalyst, as it is used for NO_x reduction in power plants and heavy-duty diesel vehicles. According to a US patent [24], MoO_3-TiO_2 should be active as an HCN hydrolysis catalyst. Molybdenum oxide was previously used as a promoter in V-catalysts, since it exhibits mild redox activities

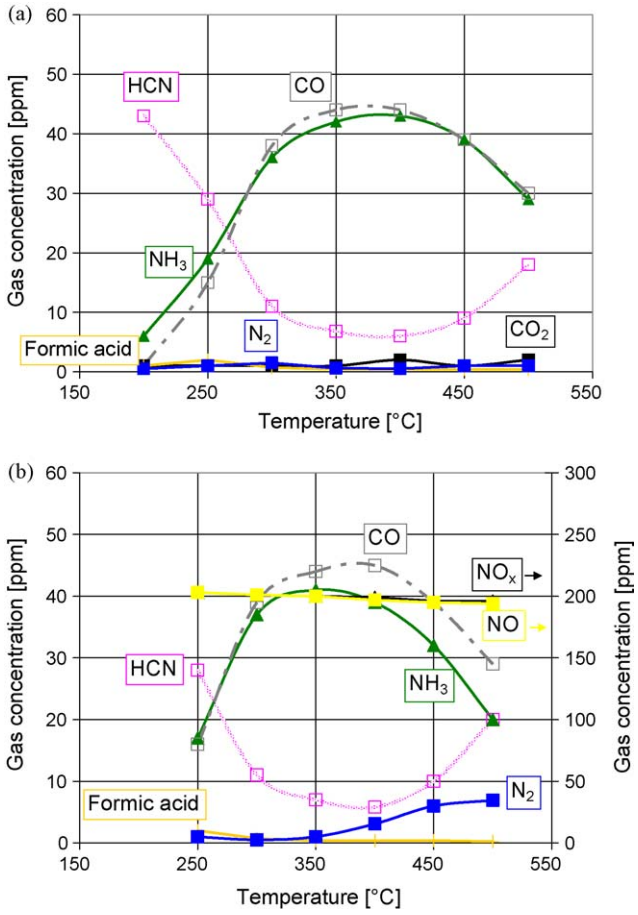

Fig. 2. HCN conversion on TiO_2 in the anatase modification. Base feed: 50 ppm HCN in N_2. GHSV = 52,000 h^{-1}. (a) 5% H_2O and 10% O_2. (b) 5% H_2O, 10% O_2 and 200 ppm NO.

Table 5
Reaction rate constants at STP of HCN decomposition over differently doped TiO_2 catalysts. Model gas: 5% H_2O, 10% O_2 and 50 ppm HCN in N_2.

$T_{cat.}$ (°C)	k_{mass} ($cm^3/(g\,s)$)					
	TiO_2	La_2O_3-TiO_2	WO_3-TiO_2	MoO_3-TiO_2	Fe_2O_3/TiO_2	V_2O_5/WO_3-TiO_2
500	279	445	126	27	239	46
450	438	682	216	25	294	49
400	504	784	237	23	424	57
350	439	660	197	21	433	58
300	306	345	121	16	291	48
250	101	105	47	11	76	27
225	–	56	–	10	51	–
200	25	27	18	10	31	13

and simultaneously increases the acidity of the support. However, its melting point is even lower than that of the vanadium oxides, and molybdenum-containing vanadia-catalysts show an increased N_2O selectivity in the SCR reaction. Finally, by supporting Fe_2O_3 on TiO_2, the influence of a weakly oxidizing redox system on HCN decomposition was examined.

3.2.1. HCN conversion rates

In Table 5 and Fig. 3, the rate constants of HCN decomposition on doped and pure TiO_2 are compared (model gas with 5% H_2O and 10% O_2).

La_2O_3-TiO_2 shows a much higher activity for the hydrolysis of HCN than pure TiO_2 at temperatures above 300 °C. At low temperatures, the activities of the two catalysts do not differ. Doping with WO_3 worsens the activity over the entire temperature range, i.e., WO_3-TiO_2 is only about half as active as TiO_2. Compared to doping with WO_3, Fe_2O_3 had an only a small negative effect on the hydrolysis properties of TiO_2. In contrast to the results in ref. [24], TiO_2 doped with MoO_3 exhibited only very low activity in our experiments. Similar weak HCN conversions were observed on the standard V_2O_5/WO_3-TiO_2 SCR catalyst. Therefore, if HCN occurs in an SCR system with a vanadia-catalyst, it cannot be destroyed over the SCR catalyst, but must be hydrolyzed upstream or oxidized downstream of the vanadia-catalyst. All doped titania catalysts exhibited the same decrease in the rate constants at high temperatures as titania, which can only be explained by a decrease in the surface coverage by one or both of the reactants H_2O and HCN [22].

3.2.2. Influence of the model gas composition

HCN conversion on the differently doped TiO_2 catalysts was not significantly affected by O_2, NO, NO_2 or NH_3. However, according to the different redox and SCR properties of the materials, the composition of the reaction products changed depending on the model gas composition (results not shown, see electronic supporting material).

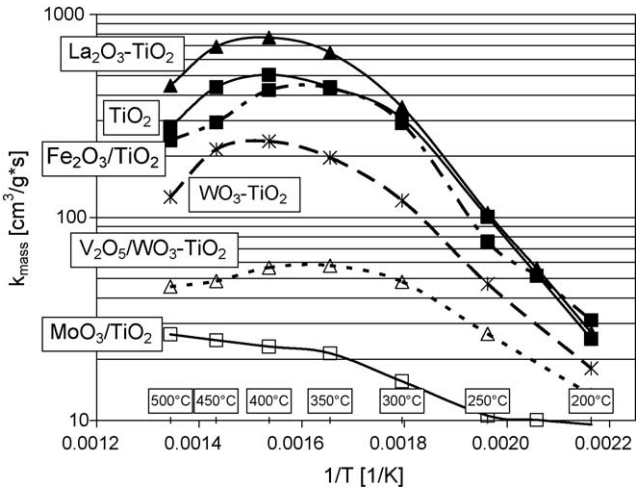

Fig. 3. Reaction rate constants at STP of HCN decomposition over differently doped TiO_2 catalysts. Model gas: 5% H_2O, 10% O_2 and 50 ppm HCN in N_2.

The hydrolysis of HCN in the presence of H_2O or H_2O/O_2 on La_2O_3-TiO_2 proceeded similarly to pure TiO_2, i.e., almost quantitative conversion to CO and NH_3. Only in the low temperature range was the formation of formic acid about twice as high as on the undoped TiO_2. When additional NO_x was dosed, part of the formed NH_3 produced N_2, as on pure TiO_2. The clearly stronger adsorption behavior of the C-reaction products on La_2O_3-TiO_2 was remarkable, which resulted in much longer equilibration times of these components upon changes in the temperature or gas concentrations. On the other hand, the NH_3 equilibrium was reached much faster. The adsorption behavior of selected catalysts will be discussed later.

Over WO_3-TiO_2, HCN was quantitatively hydrolyzed to CO and NH_3, although at a clearly lower rate than on pure TiO_2. With NO in the model gas, increasing amounts of NH_3 reacted with NO to form N_2 with increasing temperature. At 350 °C, about 50% of the generated ammonia was converted to nitrogen, and above 400 °C, almost total NH_3 conversion was reached. For NO/NO_2 dosage, the NH_3 conversion was still larger, as expected. When the dosed NO_x consisted of NO_2 only, all of the NH_3 was consumed at low temperatures, but between 400 and 500 °C, a maximum of NH_3 emission was observed. With NO_2, traces of N_2O were found in the intermediate temperature range, which is typical for NO_2-SCR [25].

On the V_2O_5/WO_3-TiO_2 catalyst, very little HCN was hydrolyzed. Since this catalyst has some oxidation capability with oxygen, only a few ppm of NH_3 were found after the catalysis with H_2O/O_2 in the feed. With NO_x in the model gas, these traces reacted completely to form N_2 due to the very high SCR activity of this catalyst, such that no more NH_3 was found in the product gas.

HCN with H_2O and O_2 was hydrolyzed over Fe_2O_3/TiO_2 to ammonia with high selectivity up to 450 °C. The increased oxidation potential of this catalyst was evident in the clearly higher formation of CO_2. The decrease in the reaction products ammonia and CO at higher temperatures might be explained by a lower surface coverage with one or both of the reactants HCN and water. When NO was dosed, a significant amount of NO_x and NH_3 was emitted along with N_2 over the entire temperature range since the catalyst showed a relatively low NO-SCR activity. The N_2 formation follows the trend of the NH_3 production since it is the product of a consecutive reaction. However, the maximum of N_2 formation was shifted to higher temperatures since the SCR activity rises more slowly than the hydrolysis activity. The slight increase in N_2 formation at 500 °C was likely caused by the oxidation of HCN, which starts to become significant at this temperature. With the dosage of NO/NO_2 at a 1:1 ratio, however, only traces of NH_3 could be found because the rest reacted to form N_2 in the fast SCR reaction, which is known to proceed efficiently over iron-based catalysts [26]. During the dosage of NO_2, CO_2 and CO were found in similar amounts up to 400 °C, but at higher temperatures CO_2 was predominantly formed.

Table 6
Reaction rate constants at STP of HCN decomposition over zeolite catalysts. Model gas: 5% H_2O, 10% O_2 and 50 ppm HCN in N_2.

$T_{cat.}$ (°C)	k_{mass} (cm³/(g s))			
	TiO_2	H-ZSM-5	Fe-ZSM-5	Cu-ZSM-5
500	279	653	1147	4648
450	438	497	843	4348
400	504	289	641	3791
350	439	138	497	2981
300	306	56	329	2510
250	101	22	102	1318
225	–	–	49	623
200	25	–	27	187

3.3. Zeolites

We were also interested in the behavior of HCN on Fe-ZSM-5 and Cu-ZSM-5 due to their application as typical SCR catalysts. H-ZSM-5 served as a reference sample of a zeolite without a redox element.

3.3.1. HCN conversion rates

Table 6 and Fig. 4 show the mass-based reaction rate constants of HCN decomposition over zeolite catalysts in comparison with pure TiO_2 (model gas with 5% H_2O and 10% O_2).

H-ZSM5 was only weakly active in the intermediate and low temperature range, and only at 500 °C was it clearly more active than TiO_2. In contrast, Fe-ZSM-5 showed exactly the same high activity as TiO_2 up to 300 °C and was even substantially more active at higher temperatures. The most important result of the catalyst screening experiments was that Cu-ZSM-5 converted HCN with an activity approximately 5–10 times higher than that of the catalysts known thus far. However, HCN was decomposed on this catalyst not by hydrolysis, but primarily by oxidation (see below). The different course of the rate constant curves of the three zeolite catalysts is shown in the Arrhenius plot in Fig. 4. H-ZSM-5 shows an almost linear rise of the rate constants, which level off only slightly at high temperatures. Fe-ZSM-5 shows a linear increase up to 300 °C, where the Arrhenius curve sharply bends and rises further at a lower rate up to 500 °C due to a conversion limitation, as the conversion approaches 90% at 300 °C.

The activity of the copper zeolite was so high that in the range between 200 and 250 °C, the rate constants do not increase linearly due to diffusion processes, which start to become predominant. This comprises gas phase diffusion onto the catalyst surface, diffusion into the catalyst layer and eventually diffusion into the pores of the zeolite. The storage behavior of Fe-ZSM-5 and Cu-ZSM-5 will be described later.

3.3.2. Influence of the model gas composition on H-ZSM-5

The influence of the model gas composition on the reaction paths and kinetics of the HCN decomposition (hydrolysis or oxidation) is very different on the zeolite catalysts, i.e., H-ZSM-5 acted as a pure hydrolysis catalyst, whereas Fe-ZSM-5 showed somewhat strong oxidation properties, and Cu-ZSM-5 was a very strong oxidant.

Due to the missing redox element of H-ZSM-5, only at very high temperatures is some HCN oxidized by O_2 (Fig. 5a). In the presence of water, the hydrolysis reaction prevailed, and quantitative conversion of HCN to NH_3 and CO was observed (Fig. 6a). With NO (Fig. 6b), NO/NO_2 (data not shown, see electronic supporting information) and NO_2 admixtures (Fig. 6c) in the feed, the formed

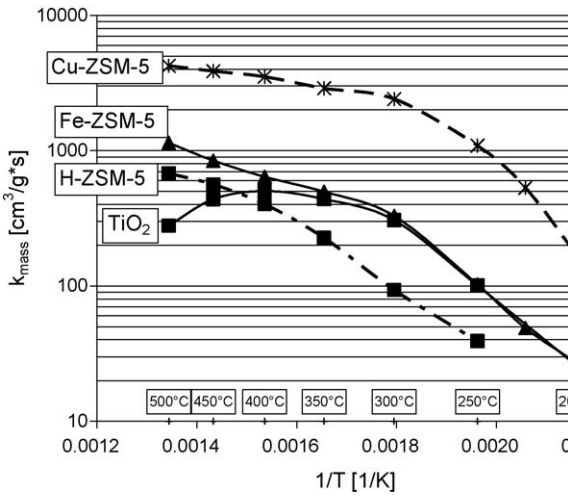

Fig. 4. Reaction rate constants at STP of HCN decomposition over zeolite catalysts. Model gas: 5% H_2O, 10% O_2 and 50 ppm HCN in N_2. GHSV = 52,000 h^{-1}.

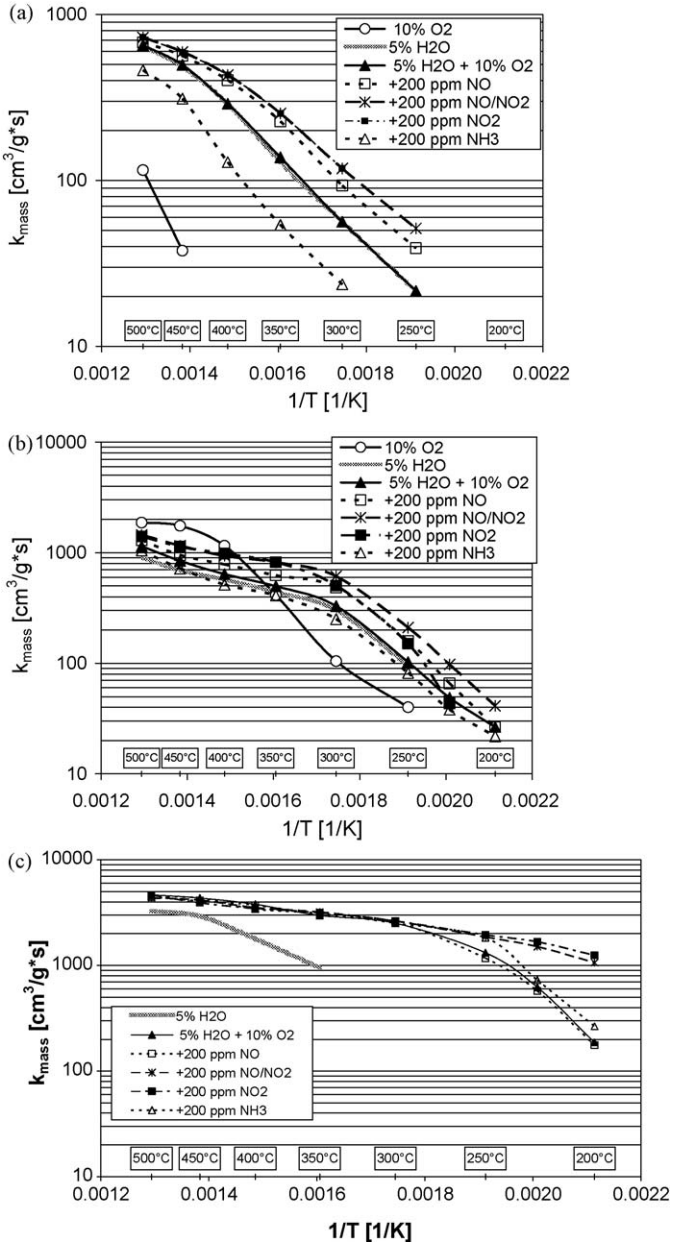

Fig. 5. Influence of the model gas composition on the rate constants of HCN conversion over (a) H-ZSM-5, (b) Fe-ZSM-5 and (c) Cu-ZSM-5.

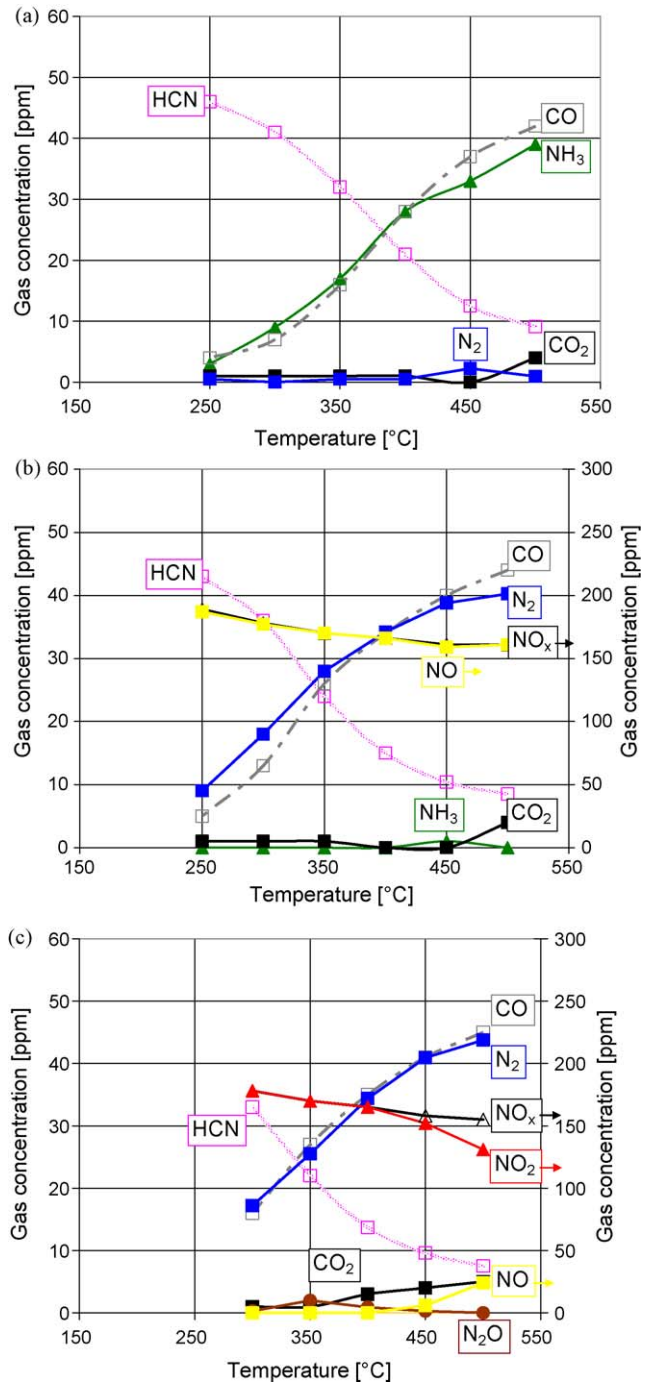

Fig. 6. HCN conversion over H-ZSM-5. Base feed: 50 ppm HCN in N_2. GHSV = 52,000 h^{-1}. (a) 5% H_2O and 10% O_2. (b) 5% H_2O, 10% O_2 and 200 ppm NO. (c) 5% H_2O, 10% O_2 and 200 ppm NO_2.

NH_3 reacted completely in the SCR reaction to form N_2. This reaction occurs rapidly (Fig. 5a), so the catalyst surface was constantly freed from the formed NH_3, which resulted in higher HCN conversions. With the dosage of NO_2, the reaction became so fast that it was twice as great as the rate constant of the HCN decomposition. NO_2 has very strong oxidizing properties, which explains the shift of the start of CO_2 formation from 500 °C when only water and oxygen were added, to 400 °C in the presence of NO_2. The thermodynamic equilibrium between NO and NO_2 lies almost completely on the side of NO at 500 °C. However, a redox element is required to convert NO_2 to NO. The few ppm of NO formed at 500 °C indicates that the catalyst started to show a low redox activity at this temperature, most likely due to iron traces, which are usually found in H-ZSM-5 samples.

When 200 ppm NH_3 was dosed, the hydrolysis of HCN was clearly inhibited on H-ZSM-5, and the activity was only half as large as without NH_3 dosage.

3.3.3. Influence of the model gas composition on Fe-ZSM-5

With oxygen in the model gas, Fe-ZSM-5 oxidized HCN to CO_2 and N_2 above 300 °C with high activity (Fig. 5b), and only at lower temperatures were traces of CO found. Since real exhaust gases always contain some water, which converts HCN via hydrolysis and inhibits oxidation, water-free experiments have rather little significance. However, the experiment did show the high oxidation capability of Fe-ZSM-5. When water was added to the feed, HCN hydrolysis started at 200 °C with almost quantitative formation of NH_3 and CO (Fig. 7a). The same HCN conversion and NH_3 selectivities were found up to 300 °C as with only water. At higher temperatures, the oxidation dominated, and CO_2 and N_2 were increasingly formed. With NO in the model gas feed, the activity of Fe-ZSM-5 was increased by oxidation of the formed NH_3 by NO in the SCR reaction to N_2 (Fig. 7b), similar to H-ZSM-5. NH_3 inhibited the HCN decomposition only slightly. The oxidation of NH_3 with NO, and at higher temperatures with O_2, proceeded very selectively to N_2. By-products such as N_2O or the additional formation of NO were not observed.

NO_2 had an even stronger promoting effect on the HCN conversion than did NO (Fig. 5 b). Again, the formed NH_3 was quantitatively consumed in the SCR reaction. At temperatures above 350 °C, the NO_2 concentration decreased at the expense of increasing NO formation over the iron redox centers. At 300 °C, the formation of a few ppm of N_2O could be observed, which is typical for NO_2- and NH_3-containing gases over Fe-ZSM-5 [27]. From HCN, NH_3 was formed over the catalyst by hydrolysis, which reacted with the NO_2 in the feed to form ammonium nitrate. Ammonium nitrate can be stably deposited on the catalyst surface at low temperatures, but decomposes to N_2O at intermediate temperatures.

3.3.4. Influence of the model gas composition on Cu-ZSM-5

Although a high GHSV of 200,000 h^{-1} was used for the test of Cu-ZSM-5, variations in the oxygen-containing model gases had an influence on the HCN conversion only at temperatures lower than 300 °C (Fig. 5c). At higher temperatures, with all model gases, almost complete HCN conversion was reached.

When only water was added to the HCN base feed, the rate constants of the HCN decomposition were clearly smaller than in the presence of oxygen. Only above 400 °C were high conversions reached with water, whereby NH_3 was formed as the main product. Instead of CO, which is the main product of HCN hydrolysis over the other catalysts in the reaction sequence HCN → methanamide → ammonium formate → formic acid → H_2O + CO, CO_2 was found, which might be formed by decarboxylation of the intermediate formic acid. In ref. [4] we have shown that for formic acid always both decomposition pathways have to be considered, depending on the catalyst and the reaction conditions. However, it cannot be certainly excluded that the CO_2 was formed by oxidation of HCN via HNCO: For the observed production of ca. 40 ppm CO_2 from HCN, only 20 ppm of O_2 in the model gas would be required — a concentration level that is easily reached as impurity in typical laboratory gases.

With O_2 and H_2O in the model gas, NH_3 and N_2 were formed on Cu-ZSM-5 between 200 and 350 °C, N_2 with traces of N_2O between 350 and 400 °C and predominantly NO above 400 °C (Fig. 8a). NO did not show a considerable influence on the rate constants of the HCN decomposition (Fig. 5c). The NH_3 formed from the HCN reacted with NO very selectively to form N_2 over the whole

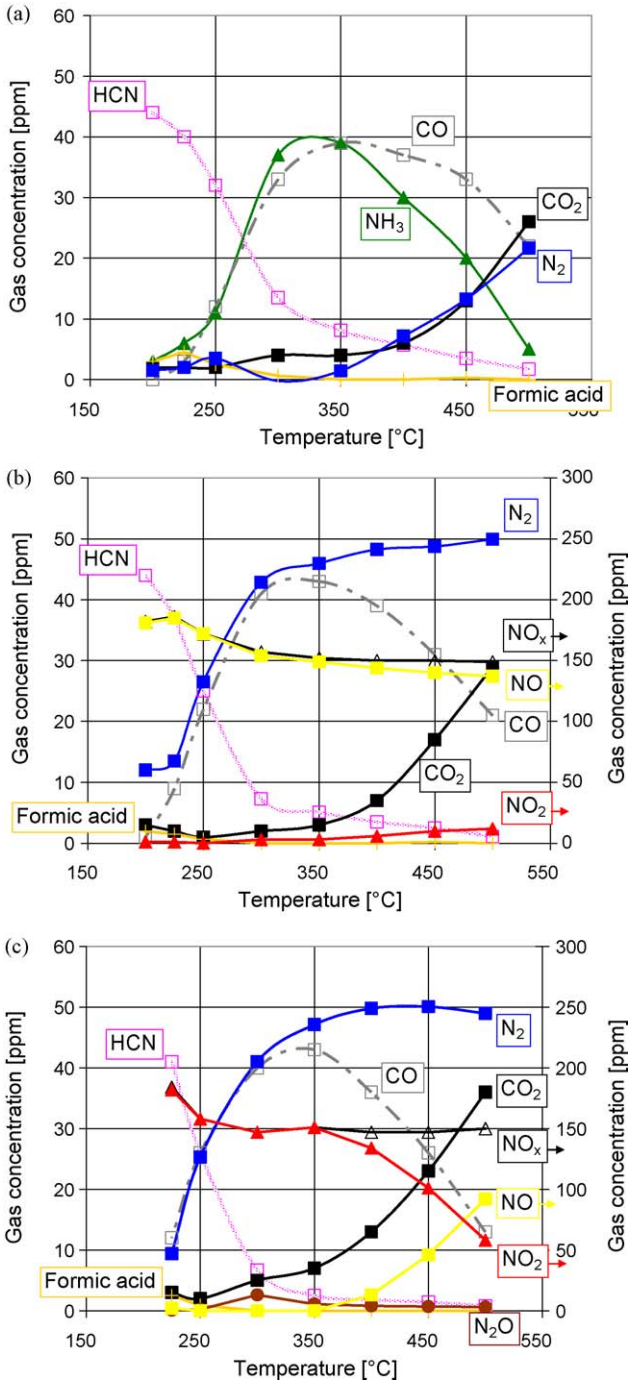

Fig. 7. HCN conversion over Fe-ZSM-5. Base feed: 50 ppm HCN in N_2. GHSV = 52,000 h^{-1}. (a) 5% H_2O and 10% O_2. (b) 5% H_2O, 10% O_2 and 200 ppm NO. (c) 5% H_2O, 10% O_2 and 200 ppm NO_2.

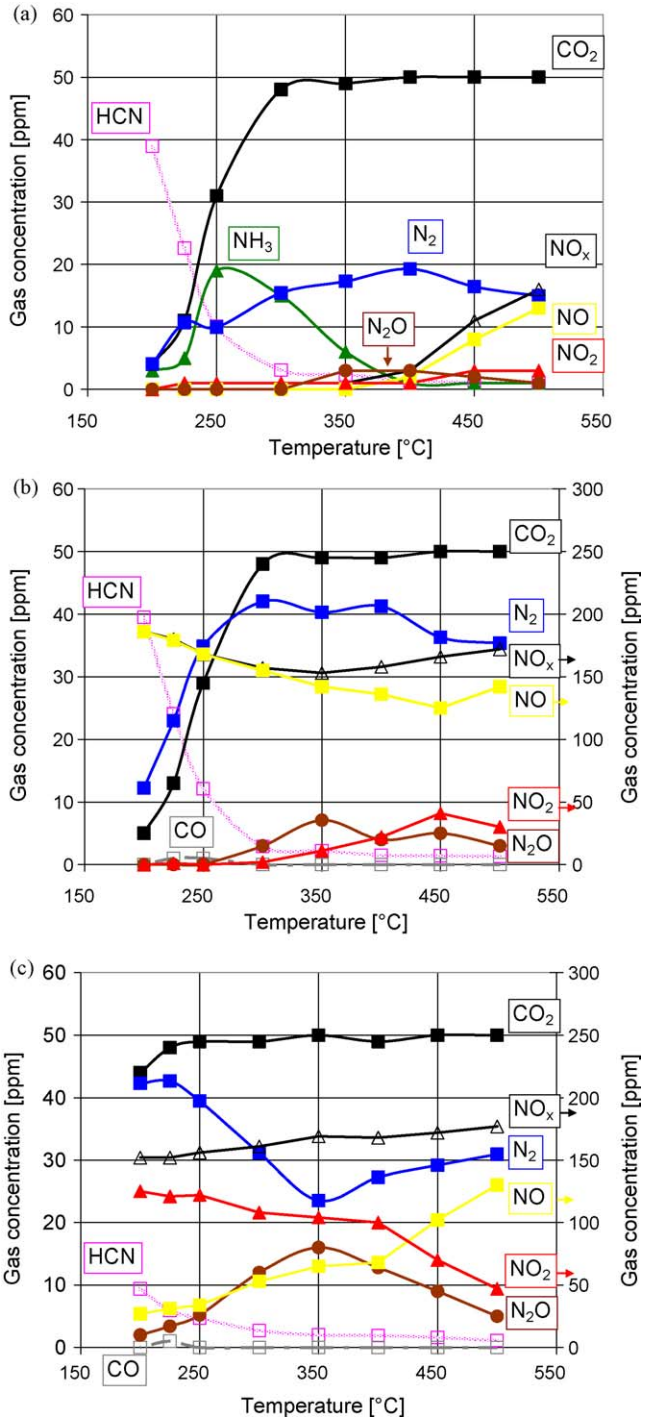

Fig. 8. HCN conversion over Cu-ZSM-5. Base feed: 50 ppm HCN in N_2. GHSV = 200,000 h^{-1}. (a) 5% H_2O and 10% O_2. (b) 5% H_2O, 10% O_2 and 200 ppm NO. (c) 5% H_2O, 10% O_2 and 200 ppm NO_2.

temperature range (Fig. 8b). Some N_2O was formed as a by-product from NH_3 at intermediate temperatures due to stronger oxidizing properties of this catalyst compared to Fe-ZSM-5 [28]. NO_2 and NO/NO_2 admixtures strongly increased the activity of the HCN decomposition in the low temperature range (Fig. 5c). At 200 °C, five-fold higher rate constants were reached, as compared with O_2 and H_2O only. In the presence of NO_2, particularly in the intermediate temperature range, N_2O was formed (Fig. 8c). The maximum of the N_2O formation was observed at 350 °C, where approximately 1/3 of the HCN was converted to N_2O and the rest to N_2. With NO/NO_2, N_2O was also formed (data not shown, see electronic supporting information), however, with a less pronounced maximum when compared with NO_2 only. When NH_3 was added to a base feed with HCN, O_2 and H_2O, NH_3 emissions were observed up to 300 °C due to both dosed and formed NH_3 (data not shown, see electronic supporting information). Above 300 °C, NH_3 was converted at a high yield to N_2, and starting from 400 °C, NO_x was increasingly formed, predominantly as NO. At 250 °C, high conversions, similar to those observed with the dosage of NO_2, were obtained. At 225 and 200 °C, the HCN conversion was lower when compared to that of the NO_2-containing gases, but it was still somewhat higher than with O_2/H_2O only.

Table 7
Mass- and volume-based rate constants at STP of HCN decomposition with 5% H_2O and 10% O_2 in the model gas.

T_{cat} (°C)	k_{mass} ($cm^3/(g\,s)$)						$k_{vol.}$ (1/s)					
	Cu-ZSM-5	Pd/Al_2O_3	Pt/Al_2O_3	$Pt/V_2O_5/WO_3$-TiO_2	Comm. DOC	MnO_x-Nb_2O_5-CeO_2	Cu-ZSM-5	Pd/Al_2O_3	Pt/Al_2O_3	$Pt/V_2O_5/WO_3$-TiO_2	Comm. DOC	MnO_x-Nb_2O_5-CeO_2
500	4648	5376	5026	527	5594	3614	600	696	650	362	615	523
450	4348	4448	3987	459	4305	3006	562	576	516	330	474	435
400	3791	4039	3355	410	3730	2490	490	523	434	290	410	360
350	2981	3313	2605	352	3168	2149	385	429	337	236	349	311
300	2510	1663	2005	295	2704	1620	324	215	260	192	297	234
250	1318	248	498	211	2228	793	170	32	64	144	245	115
225	623	118	100	103	1447	432	80	15	13	115	159	62
200	187	62	46	52	263	165	24	8	6	59	29	24

3.4. Noble-metal catalysts and MnO_x-Nb_2O_5-CeO_2

The decomposition of HCN was also investigated over a highly active commercial diesel oxidation catalyst developed for NO oxidation. It had a platinum content of 90 g Pt/ft^3, according to a platinum content of 5–6% related to the active mass.

Two model catalysts with 1% Pt and 1% Pd on Al_2O_3 were also prepared, with which the different behaviors of the two precious metals could be shown concerning activity and selectivity. Another catalyst with 1% Pt on V_2O_5/WO_3-TiO_2 corresponds to the end piece of a vanadia-based SCR catalyst, which can be impregnated with platinum to prevent NH_3 emission by oxidation. With 70 g Pt/ft^3, it exhibits a high platinum content similar to that of the commercial diesel oxidation catalyst. An MnO_x-Nb_2O_5-CeO_2 catalyst was tested due to our previous investigation of manganese-cerium mixed oxides, where it proved to be a selective redox catalyst [20]. The catalyst consists of 23 mol% manganese and niobium oxide, with the rest being cerium oxide, and proved to be very active for the SCR reaction at low temperatures and quite selective for NH_3 oxidation. Cu-ZSM-5, with its very high HCN conversion rates, was used as a reference material.

3.4.1. HCN conversion rates

In Table 7 and Fig. 9, the rate constants of HCN decomposition on the noble-metal catalysts and on MnO_x-Nb_2O_5-CeO_2 are reported in comparison to Cu-ZSM-5 (model gas with 5% H_2O and 10% O_2).

The Pd/Al_2O_3 and Pt/Al_2O_3 catalysts were very active at temperatures above 300 °C, but below 300 °C, their activity decreased significantly. At 225 and 200 °C, they were only about twice as active as undoped TiO_2. The two noble-metal-free catalysts, Cu-ZSM-5 and MnO_x-Nb_2O_5-CeO_2, showed substantially better low temperature activity. The highest activity was shown by the commercial diesel oxidation catalyst, which exhibited a very high platinum content of 5%. Due to its large mass per volume ratio, the Pt-impregnated vanadia-based SCR catalyst appeared to have a relatively low activity on the basis of mass-based rate constants, but proved to be as active as the diesel oxidation catalyst on the basis of volume-based rate constants.

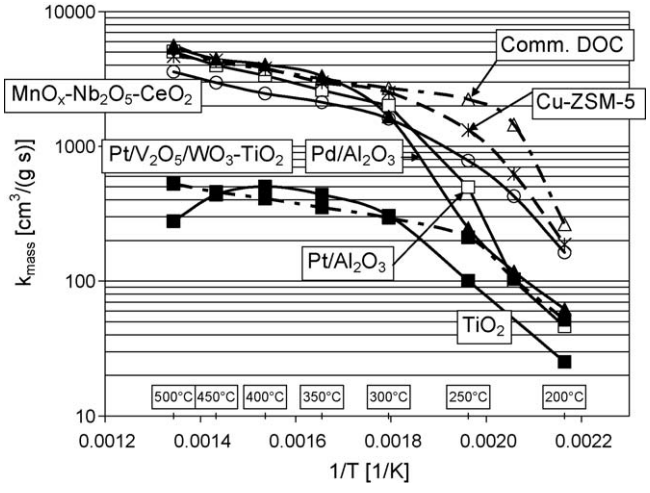

Fig. 9. Reaction rate constants at STP of HCN decomposition over Pd- and Pt-based oxidation catalysts and MnO_x-Nb_2O_5-CeO_2. Cu-ZSM-5 and TiO_2 are included as reference samples. Model gas: 5% H_2O, 10% O_2 and 50 ppm HCN in N_2.

3.4.2. Influence of the model gas composition on the activity of HCN oxidation

The influence of the model gas composition on the activity of HCN decomposition over the tested catalysts is summarized in Table 8 for $H_2O + O_2$, NO and NO_2 at 300 °C. For all other temperatures and the addition of $NO + NO_2$ and NH_3 the corresponding data can be found in the electronic supporting information.

The influence of these gases was relatively small on Pd/Al_2O_3. Compared to the model gas with O_2 and H_2O only, NO_x caused a slight inhibition of HCN oxidation at temperatures below 300 °C. In addition, NH_3 caused a clear inhibition of HCN oxidation between 250 and 300 °C. On Pt/Al_2O_3, a very strong influence of the model gas composition on the activity of HCN decomposition was observed below 350 °C. The activity was reduced by about one-half by NO_2 between 250 and 300 °C, was slightly increased by NO and was hardly affected by NO/NO_2. NH_3 slightly increased the activity at 300 °C, but strongly inhibited HCN decomposition at 250 °C. The commercial diesel oxidation catalyst and the Pt-impregnated vanadia-based SCR catalyst behaved similarly to Pt/Al_2O_3. The activity of MnO_x-Nb_2O_5-CeO_2 was affected by the model gas composition only between 200 and 250 °C. NH_3 caused a weak inhibition, and NO_2 increased the activity slightly.

3.4.3. Influence of the model gas composition on the reaction products of HCN oxidation

With O_2 and H_2O in the model gas, NH_3 and N_2 were predominantly formed on Pd/Al_2O_3, along with NO_x (Table 8). N_2O was formed mainly in the intermediate temperature range from 300 to 400 °C, with a selectivity of approximately 25%. Above 400 °C, HCN was mainly oxidized to NO_x. With NO in the model gas, a part of the formed ammonia reacted relatively selectively to form N_2 at 300 °C. At 350 and 450 °C, the laughing gas formation (S_{N_2O} = ca. 50%) was doubled, but NO_x emissions were only observed above 450 °C. With NO_2 and NO/NO_2 mixtures, all of the formed NH_3 reacted almost exclusively to form N_2 at 300 °C. The N_2O and NO formation at temperatures above 350 °C was as high as for the dosage of NO. When 200 ppm NH_3 was dosed, a N_2O maximum of 50 ppm was observed at 400 °C. At lower temperatures, the N_2 formation increased, and at higher temperatures, the NO_x formation increased.

In contrast to the Pd-catalyst, the formed NH_3 was completely oxidized over Pt/Al_2O_3 in the model gas with only O_2 and H_2O over

Table 8
Volume-based activities and selectivities at STP for HCN decomposition at 300 °C.

Catalyst	5% H_2O + 10% O_2					+200 ppm NO					+200 ppm NO_2				
	$k_{vol.}$ (1/s)	S_{NH_3} (%)	S_{NO_x} (%)	S_{N_2O} (%)	S_{N_2} (%)	$k_{vol.}$ (1/s)	S_{NH_3} (%)	S_{NO_x} (%)	S_{N_2O} (%)	S_{N_2} (%)	$k_{vol.}$ (1/s)	S_{NH_3} (%)	S_{NO_x} (%)	S_{N_2O} (%)	S_{N_2} (%)
Metal oxides, H-ZSM-5 and doped TiO_2															
TiO_2	46	92	0	0	8	46	95	3	0	3	37	86	0	0	49
Al_2O_3	12	88	0	0	13	11	80	7	0	13	10	0	0	0	264
H-ZSM-5	6	100	0	0	0	10	0	0	0	257	13	0	0	4	202
ZrO_2	3	–	–	–	–	3	–	–	–	–	3	–	–	–	–
SiO_2	1	–	–	–	–	–	–	–	–	–	–	–	–	–	–
La_2O_3-TiO_2	40	92	0	0	8	47	91	8	0	1	41	79	0	0	73
WO_3-TiO_2	18	82	0	0	18	18	86	23	0	−9	18	14	0	9	136
MoO_3/TiO_2	3	–	–	–	–	–	–	–	–	–	–	–	–	–	–
Fe_2O_3/TiO_2	41	92	3	0	5	41	78	0	0	30	43	29	0	0	145
SCR catalysts															
V_2O_5/WO_3-TiO_2	8	36	18	0	45	8	0	0	0	210	7	0	0	0	200
Fe-ZSM-5	40	101	0	0	−1	58	0	0	0	201	61	0	0	12	190
Cu-ZSM-5	324	32	2	0	66	332	0	0	13	179	340	0	0	51	132
Oxidation catalysts															
Pd/Al_2O_3	215	40	12	0	48	191	37	0	10	58	207	2	0	19	129
Pt/Al_2O_3	260	0	13	40	47	229	0	0	75	25	137	0	14	52	33
Pt/V_2O_5/WO_3-TiO_2	212	0	41	43	16	192	0	0	84	16	167	0	29	52	19
Comm. DOC	297	0	59	28	13	281	0	20	57	23	257	0	36	45	19
MnO_x-Nb_2O_5-CeO_2	203	67	9	5	19	209	22	0	5	141	226	12	0	15	134

the whole temperature range. The N_2O selectivity was somewhat higher than for the Pd-catalyst, whereby a maximum of 35–40% was reached at 250 and 300 °C. At higher temperatures, the N_2O formation decreased, but the NO_x formation strongly increased. With NO in the model gas, the N_2O formation increased by a factor of three to four between 200 and 400 °C. With NO_2 in the model gas, the N_2O formation did not significantly increase, but the N_2 formation slightly increased. The somewhat better selectivity of the Pt-catalyst, as compared to the Pd-catalyst during the dosage of NO_2, might be to due to an inhibition of the activity by NO_2.

In the model gas with HCN, O_2 and H_2O, HCN was predominantly converted to NH_3 (S_{NH_3} = ca. 90%) and N_2 on MnO_x-Nb_2O_5-CeO_2 between 200 and 300 °C. Above 350 °C, virtually all of the HCN was oxidized to NO_x. The laughing gas formation was very low, as compared to the noble-metal catalysts, with a maximum of 12% at 350 °C. Additional NO_x did not influence N_2O formation. Below 300 °C, N_2 was formed, and at higher temperatures, increasing amounts of NO_x were found.

3.5. Transient response experiments

For changes in the temperature or model gas composition, the equilibration times were unequal on the different catalyst samples. For some catalysts, the equilibrium of the C-containing reaction products was reached faster than that of the N-containing products, and vice versa. The adsorption and desorption behavior of four catalysts were examined with the following dosage and temperature change program: (1) At a constant catalyst temperature of 250 °C and with a model gas of 5% H_2O and 10% O_2, the HCN dosage was switched on and off again after 15–60 min, and equilibration was awaited. (2) After switching off the HCN dosage, weakly adsorbed components were isothermally desorbed at 250 °C for approximately 10 min. (3) The temperature was ramped from 250 to 300 °C at 10 °C/min for the desorption of more strongly adsorbed components. (4) 50 ppm HCN was adsorbed at 300 °C, and then the HCN dosage was switched off after approximately 10 min. (5) Finally, the stored reaction products were isothermally desorbed at 300 °C. For catalysts with very high NH_3 adsorption capacities, after approximately 10 min of isothermal desorption, the residual amount of stored NH_3 was measured indirectly by dosing 200 ppm NO, which consumed the stored NH_3 in the SCR reaction.

3.5.1. Transient response experiments over TiO_2

After the start of dosage at 250 °C, the HCN concentration rose rapidly to 20 ppm after the TiO_2 catalysis and reached a final concentration of approximately 30 ppm after approximately 10 min (Fig. 10a). The NH_3 emissions increased with time delay

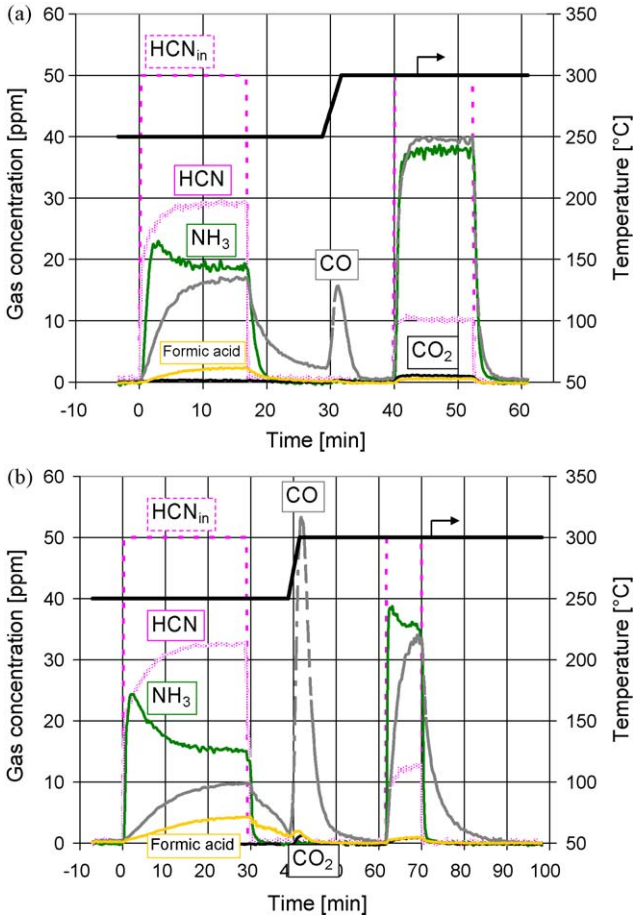

Fig. 10. Step-response experiment over (a) TiO_2 and (b) La_2O_3-TiO_2. 50 ppm HCN on and off at 250 °C, isothermal desorption at 250 °C and TPD up to 300 °C. HCN on and off at 300 °C.

to 23 ppm and finally leveled off at barely 20 ppm. The CO concentration downstream of the catalyst increased more slowly than the NH_3 concentration. The hydrolysis of HCN to ammonia and formic acid and the desorption of ammonia seemed to occur rapidly, whereas the decay of formic acid to CO and water occurred much more slowly. The balance of C- and N-species was very good shortly before the HCN dosage was stopped at 250 °C; from the dosed 50 ppm HCN, 30 ppm was emitted, and the remaining 20 ppm reacted to form 20 ppm of NH_3, 17 ppm of CO and 2–3 ppm of formic acid. After the dosage was stopped, the NH_3 production decreased quickly, whereas CO was still emitted after 10 min of desorption. Only after heating to 300 °C did the complete decomposition of the stored formic acid take place, which was visible by the steeply rising CO peak at 15 ppm and the following decrease to zero. CO is the only component that was emitted during the heating phase. At 300 °C, the rise of NH_3 and CO concentration ran in parallel and without time delay after the beginning of the HCN dosage. After 2–3 min, equilibrium was reached. After the dosage was stopped, the concentrations of NH_3 and CO went back to zero within 5 min.

3.5.2. Transient response experiments over La_2O_3-TiO_2

At 250 °C, the HCN concentration rose to 15 ppm after dosing was started and reached a final value of 32 ppm after approximately 15 min (Fig. 10b). The NH_3 concentrations showed that this slow rise was not a result of HCN adsorption and storage, but due to a slight inhibition of HCN hydrolysis by the developing reaction products. Since NH_3 adsorbed only very weakly on this catalyst, the emitted NH_3 concentration corresponded to the converted HCN concentration. Immediately after the dosage was started, the NH_3 concentration rose to approximately 25 ppm and then went back to 15 ppm, corresponding to the decrease in HCN conversion. The concentration of CO and formic acid rose only slowly after the dosage started. The C- and N-balances were good before the dosage was stopped and were within the measuring and dosing accuracy: 17–18 ppm HCN was converted to 15 ppm NH_3 and 10 ppm CO plus 4 ppm formic acid (=14 ppm C). After the dosage was stopped, the NH_3 concentration downstream of the catalyst decreased rapidly, while the concentration of CO and formic acid went back to zero after only 10 min. During the heating phase of the catalyst from 250 to 300 °C, CO evolved with a maximum of approximately 50 ppm. Even at a catalyst temperature of 300 °C, a clearly retarded rise of CO formation was observed after the start of the HCN dosage, with an accordingly slow decrease after the dosage stop.

The basic La_2O_3-TiO_2 stored very little NH_3; therefore, the decomposition of the formed formic acid proceeded more slowly in contrast to the undoped TiO_2, and furthermore, substantially larger quantities were stored on the catalyst.

3.5.3. Transient response experiments over Fe-ZSM-5

On the very acidic Fe-ZSM-5, formic acid decomposed rapidly to CO (Fig. 11a). Immediately after the dosage started, the CO concentration rose and corresponded to the converted HCN quantity. During the dosage of HCN for about 40 min, a clear decline of the decomposition reaction was observable. The HCN slip increased from approximately 25 ppm to just over 30 ppm, and the CO concentration decreased from 23 to 13 ppm, corresponding to the decrease in HCN conversion. The known high storage capacity of Fe-ZSM-5 for NH_3 was exhibited in this measurement. After 30 min of HCN dosage at 250 °C, only a few ppm of the formed 15 ppm NH_3 were found in the product gas. After the dosage stopped, the concentration of CO and formic acid decreased to zero within 10 min, and the NH_3 concentration remained unchanged at 5 ppm. During heating to 300 °C, NH_3 desorbed as a peak with a height of 65 ppm, which decreased only slowly and amounted to 10 ppm after 20 min. After the dosage was started at 300 °C, it took about 20 min to equilibrate the NH_3 concentration downstream of the catalyst. After the dosage was stopped, the NH_3 concentration decreased only slowly, and a complete and fast removal of NH_3 from the catalyst surface was only possible with the dosage of 200 ppm NO via the SCR reaction. The NO concentration at the reactor outlet only slowly approached the inlet concentration of 200 ppm during the 5 min of NO dosage due to the limited reactivity of Fe-ZSM-5 for NO-SCR at 300 °C (NO curve above concentration range of *y*-axis in Fig. 11). When the NH_3 on the catalyst surface was completely consumed part of the dosed NO was oxidized to NO_2.

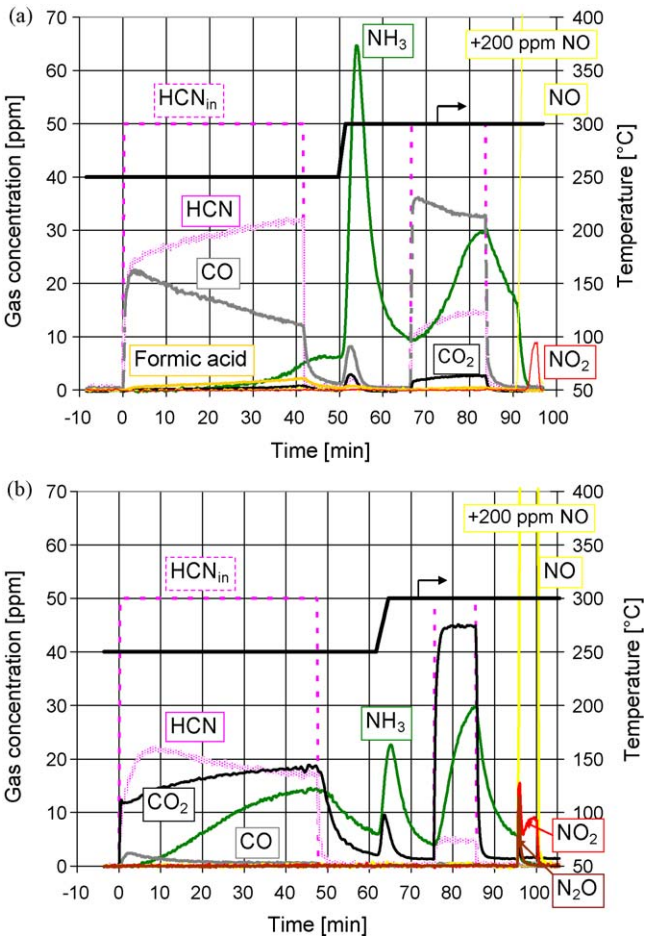

Fig. 11. Step-response experiment over (a) Fe-ZSM-5 and (b) Cu-ZSM-5. 50 ppm HCN on and off at 250 °C, isothermal desorption at 250 °C, TPD up to 300 °C, HCN on and off at 300 °C and dosage of NO for the determination of strongly adsorbed NH_3 via the SCR reaction.

3.5.4. Transient response experiments over Cu-ZSM-5

On Cu-ZSM-5, the oxidation of HCN to CO_2 took place at 250 °C, aside from the hydrolysis (Fig. 11b). The oxidation of the C^{2+} in HCN to the C^{4+} in CO_2 likely proceeded at an early reaction step of the HCN decomposition, since the oxidation of gaseous $C^{2+}O$ takes place at clearly higher temperatures on this catalyst (9% CO oxidation at 300 °C and 55% at 400 °C). The earlier rise of the NH_3 concentration after the dosage was started at 250 °C with Cu-ZSM-5, as compared to Fe-ZSM-5, is remarkable. After the dosage was stopped at 250 °C, the NH_3 concentration decreased within 10 min from 15 to 5 ppm. The NH_3 desorption peak formed during the heating phase to 300 °C is only about 1/3 as high as for Fe-ZSM-5. In the NO dosage phase from t = 95–100 min, NO_2 was instantaneously found at the reactor outlet due to the high oxidizing capability of Cu in the zeolite. The resulting NO/NO_2 mixture

quickly consumed the residual adsorbed NH_3 in the SCR reaction in accordance with the very high SCR reactivity of Cu-ZSM-5. The consumption of NH_3 was accompanied by the parallel formation of N_2O in a sharp peak, since the pronounced redox properties of copper in Cu-ZSM-5 do not only result in high SCR activity but also in unselective oxidation of NH_3 to N_2 and N_2O [19].

At a first glance, the lower NH_3 storage capacity of Cu-ZSM-5 seems to be in contrast to previous studies of the SCR reaction on these materials, in which Cu-ZSM-5 showed a higher storage capacity than Fe-zeolites, especially at low temperatures [29–31]. However, a balance of the stored amount of NH_3 via NH_3 slip was not possible due to the above mentioned high NH_3 oxidation rate over Cu-ZSM-5 to N_2. A possible reason for the unexpectedly low amount of adsorbed NH_3 on Cu-ZSM-5 could be a competitive adsorption of CO (or cyanide) on the same sites, since CO is known to adsorb on Cu-ZSM-5, especially when the Cu is in the oxidation state +1. This explanation is supported by the significant deficit in the carbon balance, observable in Fig. 11b during the dosage of HCN.

At 300 °C, the CO_2 formation equilibrated 2–3 min after the start of the HCN dosage, whereas NH_3 needed approximately 10 min. The C-balances were very good at 300 °C; from the 50 ppm HCN dosed, 5 ppm was emitted, and the observed 45 ppm CO_2 corresponds to the converted 45 ppm HCN. From the formed NH_3, only 30 ppm was found downstream of the catalyst, and the rest was oxidized to N_2.

The analysis of the measuring results revealed traces of HNCO in the product gas (Fig. 12). This is an important observation that helps to explain both the high reaction rates of the HCN decomposition as well as the formation of CO_2 over Cu-ZSM-5. In an initial step, HCN was oxidized to HNCO (15), which then hydrolyzed with very high reaction rates to NH_3 and CO_2. The hydrolysis of HNCO starts with the addition of water and the formation of carbamic acid as an intermediate, which instantaneously decomposes under the conditions applied to CO_2 and NH_3 [32].

$$HCN + 1/2O_2 \rightarrow HNCO \quad (15)$$

$$HNCO + H_2O \rightarrow H_2NC(O)OH \rightarrow CO_2 + NH_3 \quad (16)$$

This explanation is in line with the results of Solymosi and Berko, who suggested that the oxidation of adsorbed CN species proceed via isocyanate species to CO_2 on Cu(1 1 1) [33]. Conversely, on Fe-ZSM-5 and the two TiO_2-containing catalysts, the formation of both HNCO and CO_2 was not observed (except for some traces of CO_2 on Fe-ZSM-5 at 300 °C), which is in line with a HCN decomposition mechanism that occurs primarily via hydrolysis to NH_3 and CO.

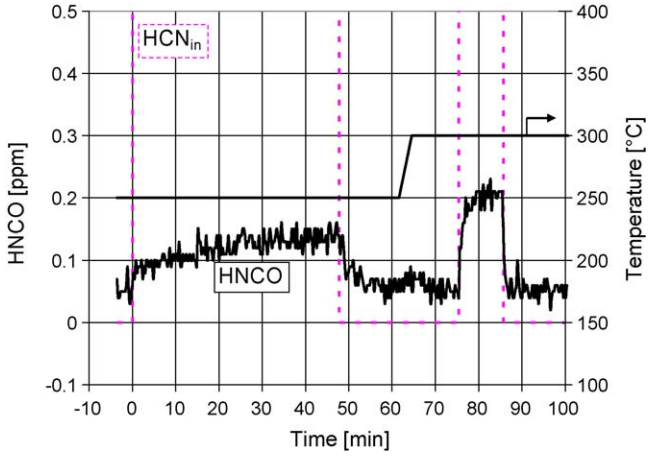

Fig. 12. HNCO concentration during the step-response experiments over Cu-ZSM-5.

4. Discussion

When closely examining the reaction network of the heterogeneous decomposition of HCN, two main reaction pathways must be distinguished. The pure hydrolysis catalysts, such as TiO_2 or Al_2O_3, formed NH_3 and CO in high yield. The occurrence of formic acid on these catalysts shows that HCN hydrolysis must have taken place at low temperatures in at least two stages via hydrolysis of methanamide to NH_3 and formic acid. Methanamide as an intermediate product was not found in our measurements, but this was also not expected due to our experiences from a previous study of the hydrolysis of methanamide [4]. The hydrolysis of methanamide occurs much more rapidly than that of HCN, so it would react immediately and cannot accumulate to detectable concentrations.

On the basis of our results, it cannot be concluded whether the direct thermolysis of methanamide to NH_3 and CO plays a role under humid reaction conditions as postulated in [16]. This should be the subject of further experiments with a typical hydrolysis catalyst under water-free conditions. However, under consideration of the relatively high stability of methanamide upon heating and the rather low temperature at which methanamide hydrolysis to formic acid was observed, it is rather unlikely that direct thermolysis of methanamide significantly contributes to its conversion to NH_3 and CO.

The oxidizing catalysts in this study, such as Pt/Al_2O_3 or Cu-ZSM-5, exhibited a substantially higher activity for HCN decomposition than did pure hydrolysis catalysts. In addition to CO_2, the typical reaction products of NH_3 oxidation are formed, but NH_3 itself is also formed at low temperatures. The formation of ammonia shows that one reaction step of HCN decomposition must also be hydrolysis on these catalysts. In ref. [16], the formation of cyanogen $(CN)_2$ was observed during the decomposition of HCN in a dry model gas over Cu-ZSM-5 at 270 °C, while in our measurements with water in the model gas, traces of HNCO were found. Cyanogen in water behaves like elementary halogens since the two C^{3+} atoms in cyanogen disproportionate to a C^{2+} (hydrocyanic acid) and C^{4+} (isocyanic acid) (17) [34]. The formed isocyanic acid hydrolyzes very easily with water to NH_3 and CO_2 (18).

$$(C^{3+}N)_2 + H_2O \rightarrow HC^{2+}N + HNC^{4+}O \quad (17)$$

$$HNCO + H_2O \rightarrow NH_3 + CO_2 \quad (18)$$

This indicates a two-stage reaction mechanism of HCN decomposition on Cu-ZSM-5 with (a) the oxidation of the C-atom to C^{4+}, either directly to HNCO/cyanate or via the formation of cyanogen and disproportionation, and (b) the hydrolysis of HNCO/cyanate to NH_3 and CO_2.

In addition, on the precious-metal-based catalysts, the hydrolysis of HCN oxidation products might play an important role. Thus, NH_3 was formed over the Pd-containing catalyst up to 300 °C, which is only possible with a hydrolysis step. For higher temperatures or other precious-metal-based oxidation catalysts, where NH_3 formation was not observed, the same reaction products were formed as for the oxidation of NH_3, with the expected N_2O selectivities, which confirms the occurrence of a hydrolysis step in the reaction sequence.

The discussed possible reaction pathways of HCN in oxygen- and/or water-containing atmospheres over the different catalysts are summarized in Fig. 13. For the sake of clarity and simplicity, the reaction network is depicted with hydrogen-saturated molecules, whereas the real situation on the catalyst surface would be better represented by a formulation of adsorbed species.

In the presence of water, only the hydrolysis of HCN to NH_3 and CO can take place, which is shown in the right branch of Fig. 13. The

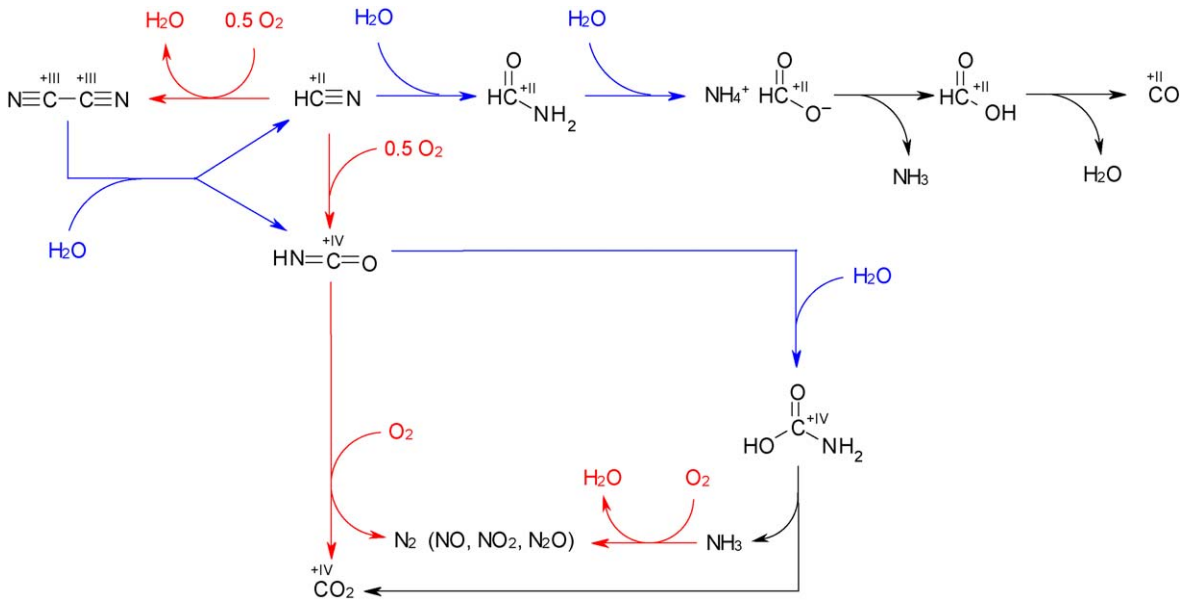

Fig. 13. Possible reaction pathways of the heterogeneous decomposition of HCN in the gas phase. (▬) Oxidation. (▬) Hydrolysis. (▬) Thermolysis.

occasionally observed emission of formic acid suggests that the mechanism of hydrolysis involves the formation of methanamide and ammonium formate, which finally decomposes to ammonia and formic acid. The formic acid itself thermolyzes further to water and CO. This reaction sequence is also typical for pure hydrolysis catalysts, such as TiO_2, which exclusively catalyzes this reaction sequence, even in the presence of oxygen. Cant et al. found that methanamide may also directly decompose to NH_3 and CO in the absence of water over metal-exchanged zeolites at temperatures above 250 °C [15]. However, this reaction is regarded as less plausible under the conditions of this study due to the relatively high thermal stability of methanamide and its ready hydrolysis to ammonia and formic acid in the presence of water as described in ref. [4].

In the presence of oxygen, HCN can only be directly oxidized to CO_2 and N_2 (plus NO, NO_2 and N_2O as side-products), following the top-down reaction sequence via isocyanic acid (HNCO) as an intermediate. However, it is rather unlikely that this straightforward sequence plays a role in the presence of oxygen and water, even for typical oxidation catalysts such as Pt/Al_2O_3 or Cu-ZSM-5. When water is also present with oxygen, the hydrolysis of the intermediate isocyanic acid to ammonia and CO_2 is preferred, as compared to its direct oxidation. Since, on a strong oxidation catalyst, ammonia can be easily further oxidized, the final products are the same, i.e., nitrogen plus the side-products NO, NO_2 and N_2O, depending on the reaction conditions. Another intermediate, which must be considered under oxidizing conditions in the reaction network, is cyanogen $(CN)_2$. The formation of this compound is easily possible by the oxidation of HCN on platinum- and copper-based catalysts, but it also efficiently reacts with water in a disproportionation reaction to HCN and HNCO. Since the formation of cyanogen is reported on platinum, copper and other catalysts under reaction conditions similar to those applied in our study, an appropriate reaction sequence was considered in our scheme.

5. Summary and conclusions

Among the tested hydrolysis catalysts, the amphoteric TiO_2 samples proved to be best suited for the decomposition of HCN to NH_3 and CO. Al_2O_3 may also be used as a hydrolysis catalyst, but the activity was about 50% lower. ZrO_2 was only slightly active, and SiO_2 was virtually inactive. La_2O_3-TiO_2 showed a higher HCN hydrolysis activity than did undoped TiO_2 at high temperatures, but it also exhibited a higher storage capacity for formic acid and a higher formic acid slip at low catalyst temperatures due to its basic surface. The doping of TiO_2 with acidic oxides markedly decreases the activity of HCN decomposition, i.e., WO_3-TiO_2 as the standard base material for the production of vanadia SCR catalysts is only half as active as undoped TiO_2. The doping of TiO_2 with Fe as a weakly oxidizing redox element did not result in any advantages. The hydrolysis characteristics changed only slightly but, at high catalyst temperatures, more NH_3 was oxidized by O_2, and, at low temperatures, a small increase in the formation of formic acid was observed. The catalytic hydrolysis proceeded quantitatively to NH_3 and CO via methanamide, ammonium formate and formic acid as intermediates.

The V_2O_5/WO_3-TiO_2 catalyst showed virtually no HCN hydrolysis activity and is therefore not suitable for the elimination of HCN from exhaust gas. This means that if HCN is formed in an engine equipped with a vanadia-based SCR catalyst, it must be hydrolyzed before it enters the SCR catalyst or it must be oxidized on a downstream oxidation catalyst.

H-ZSM-5 exhibited only low HCN hydrolysis activity, which was strongly influenced by other gas components. NH_3 strongly inhibited HCN decomposition, but NO and NO_2 increased HCN conversion, as the formed NH_3 reacted with the NO_x and cleaned the catalyst surface through the SCR reaction. The catalyst showed a relatively high SCR activity, but only at low NH_3 concentrations.

On Fe-ZSM-5, HCN was converted to ammonia above 300 °C without any problem, and in the presence of NO, it was also converted by the SCR reaction to N_2. In contrast to SCR systems with vanadia-catalysts, those with Fe-ZSM-5 should be able to cope with small HCN concentrations and it may be operated as a SCR catalyst without any additional measures in the presence of HCN in the feed gas, since HCN is hydrolyzed to NH_3 over this catalyst with similar activity as over TiO_2. As the NO_x in real exhaust gas will react with the NH_3 produced from HCN over Fe-ZSM-5 to form harmless nitrogen, HCN can be regarded as a SCR "reducing agent" when used with an Fe-zeolite catalyst. If necessary, the space velocity can be reduced to fulfill the double function as SCR and HCN hydrolysis catalyst.

The Cu-ZSM-5 catalyst converted HCN with 5–10 times higher activity than did Fe-ZSM-5 or TiO_2, but it was a NH_3 slip catalyst rather than an SCR catalyst at temperatures above 250 °C due to its high ammonia oxidation activity. HCN was oxidized very selectively to N_2 over this catalyst, particularly in the presence of NO. Although, with an increasing NO_2 fraction in the NO_x, the tendency for the formation of laughing gas rose, it was substantially lower than that obtained on precious-metal-based catalysts. NO_2 in the model gas strongly increased HCN conversion at 200 and 250 °C. At 200 °C, it was about twice as high as that obtained with the platinum-based commercial diesel oxidation catalyst and approximately ten times higher than that observed with 1% Pt on Al_2O_3.

The Pd- and Pt-containing catalysts oxidized HCN at temperatures above 300 °C with similarly high activity but with clearly higher N_2O formation than Cu-ZSM5 or MnO_x-Nb_2O_5-CeO_2. Below 300 °C, their activity was lower. The commercial platinum-based diesel oxidation catalyst and the Pt-impregnated vanadia-based SCR catalyst behaved very similarly to Pt/Al_2O_3. Pt/Al_2O_3 was somewhat more active than Pd/Al_2O_3, but it formed predominantly N_2O instead of N_2 between 200 and 350 °C and, with increasing temperature, formed NO_x.

Although palladium- and platinum-containing oxidation catalysts proved to be highly active for the oxidation of HCN above 250–300 °C, they cannot be recommended as HCN oxidation catalysts since the same unwanted side-products are formed as in the oxidation of NH_3, i.e., aside from nitrogen NO, NO_2 and N_2O may be formed. The observed high selectivity of all of the tested precious-metal-based oxidation catalysts for the formation of N_2O from ammonia is a known drawback of this catalyst type [35], which renders their application as oxidation catalysts in an HCN- or NH_3-containing exhaust gas questionable [36].

On MnO_x-Nb_2O_5-CeO_2, HCN was decomposed primarily to NH_3 up to 300 °C and, in the presence of NO_x, with a high selectivity to N_2. Above 300 °C, HCN was preferentially oxidized to NO_x. The N_2O formation on MnO_x-Nb_2O_5-CeO_2 was five times smaller than on the precious-metal-based catalysts.

In contrast to the precious-metal containing catalyst, Cu-ZSM-5 and MnO_x-Nb_2O_5-CeO_2 are well suited as HCN oxidation catalysts and can oxidize HCN with high activity and good selectivity to N_2. Moreover, these catalysts do not contain expensive noble metals, which renders their application in diesel exhaust gas treatment systems more economically favorable. In the presence of oxygen and water, a combination of oxidation and hydrolysis steps occurs, involving the formation of cyanates that hydrolyze through carbamates to CO_2 and ammonia. The intermediate ammonia is then oxidized to N_2, NO, NO_2 and N_2O with the same selectivities as the oxidation of NH_3. The formation of cyanogen from HCN, followed by its hydrolysis to HCN and HNCO, might play a role in the HCN reaction pathways with water and oxygen over Pd-, Pt- and Cu-containing catalysts.

Appendix A. Supplementary data

Supplementary data associated with this article can be found, in the online version, at doi:10.1016/j.apcatb.2009.07.021.

References

[1] H.L. Karlsson, Sci. Total Environ. 334–335 (2004) 125.
[2] F. Radtke, R.A. Koeppel, A. Baiker, Appl. Catal. A 107 (1994) L125.
[3] I.O.Y. Liu, N.W. Cant, M. Kögel, T. Turek, Catal. Lett. 63 (1999) 241.
[4] O. Kröcher, M. Elsener, E. Jacob, Appl. Catal. B 88 (2009) 66.
[5] O. Kröcher, M. Elsener, E. Jacob, 5th International Exhaust Gas and Particulate Emissions Forum, 19–20 February 2008, Ludwigsburg (Germany), http://ega.web.psi.ch/Krocher_Emission_Forum 2008.pdf.
[6] R.F. Carpenter, S.E. Linder, J. Soc. Chem. Ind. 24 (1905) 63.
[7] J.D.F. Marsh, W.B.S. Newling, J. Rich, J. Appl. Chem. 2 (1952) 681.
[8] T. Miyadera, Appl. Catal. B 16 (1998) 155.
[9] J.W. Hoard, A.P. Panov, SAE Technical Paper Series 2001-01-3512.
[10] H. Zhao, R.G. Tonkyn, S.E. Barlow, B.E. Koel, C.H.F. Peden, Appl. Catal. B 65 (2006) 282.
[11] P.L. Hagans, X. Guo, I. Chorkendorff, A. Winkler, H. Siddiqui, J.T. Yates Jr., Surf. Sci. 203 (1988) 1.
[12] X. Guo, A. Winkler, I. Chorkendorff, P.L. Hagans, H.R. Siddique, J.T. Yates Jr., Surf. Sci. 203 (1988) 17.
[13] R.H. Fahnenstich, W.Th. Heimberger, F.M. Theissen, W.M. Weigert, Chem. Ztg. 96 (1972) 388.
[14] T. Nanba, A. Obuchi, S. Akaratiwa, S. Liu, J. Uchisawa, S. Kushiyama, Chem. Lett. 29 (2000) 986.
[15] N.W. Cant, A.D. Cowan, I.O.Y. Liu, A. Satsuma, Catal. Today 54 (1999) 473.
[16] N.W. Cant, I.O.Y. Liu, Catal. Today 63 (2000) 133.
[17] I.O.Y. Liu, N.W. Cant, Catal. Surv. Asia 7 (2003) 191.
[18] I.O.Y. Liu, N.W. Cant, J. Catal. 195 (2000) 352.
[19] O. Kröcher, Stud. Surf. Sci. Catal. 171 (2007) 261.
[20] M. Casapu, O. Kröcher, M. Elsener, Appl. Catal. B 88 (2009) 413.
[21] M. Koebel, M. Elsener, Chem. Eng. Sci. 53 (1998) 657.
[22] M. Kleemann, M. Elsener, M. Koebel, A. Wokaun, Ind. Eng. Chem. Res. 39 (2000) 4120.
[23] G. Piazzesi, The catalytic hydrolysis of isocyanic acid (HNCO) in the urea-SCR process, Ph.D. thesis No. 16693, ETH Zurich, Switzerland, 2006, http://ega.web.psi.ch/Piazzesi, PhD thesis, ETH Zurich, 2006.pdf.
[24] R.J. Koveal, S.C. Leviness, US Patent 6107353 (2000).
[25] G. Madia, M. Koebel, M. Elsener, A. Wokaun, Ind. Eng. Chem. Res. 41 (2002) 4008.
[26] A. Kato, S. Matsuda, T. Kamo, F. Nakajima, H. Kuroda, T. Narita, J. Phys. Chem. 85 (1981) 4099.
[27] S. Brandenberger, O. Kröcher, A. Tissler, R. Althoff, Catal. Rev. Sci. Eng. 50 (2008) 492.
[28] O. Kröcher, M. Elsener, Ind. Eng. Chem. Res. 47 (2008) 8588.
[29] S.J. Schmieg, J.-H. Lee, SAE Technical Paper Series 2005-01-3881.
[30] H. Sjövall, R.J. Blint, L. Olsson, J. Phys. Chem. C 113 (2009) 1393.
[31] O. Kröcher, M. Devadas, M. Elsener, A. Wokaun, N. Söger, M. Pfeifer, Y. Demel, L. Mussmann, Appl. Catal. B 66 (2006) 208.
[32] I. Czekaj, O. Kröcher, G. Piazzesi, D.F.T. Calculations, J. Mol. Catal. A 280 (2008) 68.
[33] F. Solymosi, A. Berko, Surf. Sci. 122 (1982) 275.
[34] G.J. Janz, Inorg. Syn. 5 (1957) 43.
[35] Y. Li, J.N. Armor, Appl. Catal. B 13 (1997) 131.
[36] H. Suzuki, H. Ishii, JSAE Paper No. 20085606.